Physics Letters A 377 (2013) 1720–1724

Contents lists available at SciVerse ScienceDirect

Physics Letters A

www.elsevier.com/locate/pla

A theoretical study of the spectral shifts of Xe atom in Ar environment

Marcelo Hidalgo, Sylvio Canuto *

Instituto de Física, Universidade de São Paulo, CP 66318, 05314-970, São Paulo, SP, Brazil

ARTICLE INFO

Article history:
Received 25 February 2013
Received in revised form 30 April 2013
Accepted 2 May 2013
Available online 13 May 2013
Communicated by C.R. Doering

Keywords:
Liquid simulation
Atomic spectroscopy
Rare-gas liquids
Spectral shifts
Solvent effects

ABSTRACT

Liquid configurations generated by Metropolis Monte Carlo simulations are used in time-dependent density functional theory calculations of the spectral line shifts of atomic impurities in rare-gas environment. Consistent results are obtained for the Xe $5p \rightarrow 6s$ excitation in Ar environment in all thermodynamic conditions considered, with densities varying from 0.15 to 1.40 g/cm^3, thus ranging from the low to the high-density situation, including supercritical condition. The results reproduce very well the dependence of the spectral shift with the density, giving also good quantitative results for the low, intermediate and high-density cases.

1. Introduction

The Xe–Ar is one of the most important cases of liquids composed by rare-gas atoms, and exemplifies an impurity state in condensed phase. The theoretical study of such systems is a challenge for present quantum chemical methods. The most natural approach is the use of methods for dealing with solvent effects. In the last decade we have witnessed a large advance in the theoretical description of solvent effects in molecular and bio-molecular systems [1,2]. This is a natural consequence of the simple fact that most spectroscopic studies of organic molecules are in solution or are diluted in a specific solvent. Theoretical methodologies have then been developed and great progress has been obtained with continuum models [1,3], where the solvent is described in some average way and represented by its macroscopic constants. Because of its simplicity it is the method of choice, used in several applications. There are, however, known limitations and the two most usually quoted are (i) the difficulties in dealing with specific interactions and (ii) the lack of a proper thermodynamic, hence statistical, condition. There is another one that may be crucial when dealing with atomic systems. Neutral atoms lacking the electrostatic moments become a great problem for the continuum methods. The interaction involving the environment and the reference atom is thus non-electrostatic such as dispersion and exchange. This is the case of neutral Xe and Ar atoms where all the electrostatic moments are null (charge, dipole, quadrupole, octopole moments, etc.). An alternative that has also attracted attention is the standard bubble model [4,5], but this lacks a detailed consideration of the thermodynamic condition. This challenging situation requires the explicit use of the environment atoms interacting to one another and with the reference impurity atom. In addition, as the results depend on the thermodynamic condition a proper consideration of the liquid state must be used. The combined and sequential use of liquid simulation and quantum mechanics can meet these requirements. A simulation of the liquid (such as Monte Carlo or molecular dynamics) can be performed in the proper thermodynamic condition and the subsequent use of quantum mechanics (QM) can be performed in sampled configurations. The properties are statistical averages and it is important to ensure statistical convergence. This sequential use of Monte Carlo and quantum mechanics has been successfully used to describe molecular properties in different solvents [6–8], including the supercritical condition [9].

In this study we are interested in describing the low-lying excited states of Xe ($^1P_1$ and $^3P_1$) in Ar (^1S_o) environment. Previous experimental studies were performed for Xe in different thermodynamic conditions of liquid Ar. These include normal liquids as well as supercritical fluids, above the critical point ($T = 150.8$ K, $P = 48.1$ atm). The condition we aim here is the excited state impurity in a rare-gas liquid or supercritical fluid. This may be of interest also in giving some basic understanding for the development of the green chemistry where solvents are replaced by supercritical fluids, less harmful to the environment. The absorption spectrum of low pressure Xe gas very clearly exhibits the known doublet [10]: the singlet $^1S_o \rightarrow {}^1P_1$ and triplet $^1S_o \rightarrow {}^3P_1$ transitions, located at 130 nm and 147 nm, respectively. It is known experimentally that both transitions in Ar environment suffer a blue shift compared to the gas phase situation [10–12]. The size of the blue

* Corresponding author. Tel.: +55 11 3091 6805; fax: +55 11 3814 0503.
E-mail address: canuto@if.usp.br (S. Canuto).

0375-9601/$ – see front matter
http://dx.doi.org/10.1016/j.physleta.2013.05.008

shift depends on the thermodynamic condition and increases with the density. For very low densities (below ~ 0.2 g/cm^3) the shift becomes very small and negative before turning into zero [11]. For instance, if $T = 93$ K and $P = 142$ atm (corresponding to a density of 1.40 g/cm^3) the $^1S_0 \rightarrow {}^3P_1$ transition is located at 0.4 eV to the higher energy side, compared to the same transition in Xe gas. The nature of this shift has been of interest for some time and has been studied by different approaches [10–13]. In this work we will initially focus on describing the electronic excitations of Xe in Ar environment in the above thermodynamic condition. Later on we will consider also other situations and will analyze the spectral shifts as a function of the liquid density. In line with the experiments available these thermodynamic conditions cover low, intermediate and high-density regimes with some entering into the supercritical region [11]. We will then consider six thermodynamic situations corresponding to densities varying from 0.15 to 1.40 g/cm^3. We will make special consideration for the case of 0.15 g/cm^3 where the shift may change sign.

2. Methods

A proper treatment of liquid systems should consider its statistical nature [14] as there are many possible geometrical arrangements accessible to the system at nonzero temperature. Thus, liquid properties are best described by a statistical distribution [6–8,14], and all properties are obtained from statistical averages. It is thus important the use of statistical mechanics, with some sort of computer simulation of liquids [6–9], combined with quantum mechanics to obtain the electronic properties of interest.

In this Letter we use the sequential Monte Carlo quantum mechanics (S-MC/QM) methodology ([6], see also Chapter 7 of Ref. [2]). We first generate the structure of the liquid using Metropolis Monte Carlo. Next, statistically relevant configurations are systematically sampled for the quantum mechanical calculations. Several QM calculations are necessary to obtain the ensemble average that is necessary to characterize the statistical nature of the liquid. We sample statistically uncorrelated configurations [6–9] and statistically converged results are obtained in all cases.

The Monte Carlo (MC) simulations are performed in the *NVT* ensemble [15] which is more convenient for the analysis of the results as a function of the density. We use the image method combined with the periodic boundary conditions of a cubic box [15]. We use one Xe atom surrounded by 500 Ar atoms. In the case of $\rho = 1.4$ g/cm^3, for instance, this corresponds to a cubic box of size $L = 28.8$ Å. The atoms interact by the conventional Lennard–Jones potential with parameters $\varepsilon = 0.2339$ kcal/mol and $\sigma = 3.401$ Å for Ar and $\varepsilon = 0.4330$ kcal/mol and $\sigma = 3.935$ Å for Xe, as suggested by Verlet and Weis [16]. All MC simulations were performed with the DICE program [17]. After the MC simulation, 150 statistically uncorrelated configurations [6–9] are separated for the subsequent QM calculations. These configurations are composed of the central Xe atom surrounded by 13 explicit Ar atoms, corresponding to the first solvation shell in the thermodynamic condition of $T = 151$ K and density $\rho = 1.05$ g/cm^3. The use of the Xe + 13Ar configurations in the QM calculations allows the wave function to delocalize over the impurity and the environment.

Quantum mechanical calculations are then performed on these configurations generated by the MC simulations. Six different thermodynamic conditions are used, with a systematic change in the density but corresponding to actual experimental conditions used. In each case 150 QM calculations are performed to ensure statistical convergence. Hence, this study reports the result of 900 QM calculations. In every case considered the experimental bands are relatively broad [11] and do not resolve the different components of the ^1P or ^3P states. The line broadening will also be considered in this theoretical study. All QM calculations are made at

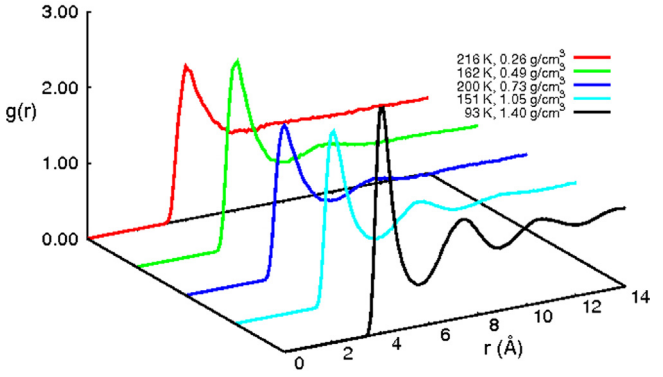

Fig. 1. Pair-wise Xe–Ar radial distribution functions for different thermodynamic conditions.

the time-dependent density functional theory (TDDFT) [18]. We have used the Becke three-parameter functional [19] with the exchange correlation due to Lee, Yang and Parr [20], combined with the SDD effective-core potential basis set [21,22], B3LYP/SDD. The SDD basis in the effective core potential approximation includes one-component relativistic energy correction [22]. The use of two dispersion-corrected DFT, the B97-D [23] and ωB97X-D [24] functionals, will also be considered for comparison and the results briefly discussed. All QM calculations were made using the Gaussian 09 program [25].

3. Results and discussions

We first analyze the distribution of Ar around the central Xe atom. Fig. 1 shows the pair-wise radial distribution function exhibiting the coordination of Ar atoms. The first is the case of $T = 93$ K and $\rho = 1.40$ g/cm^3 experimentally [11] corresponding to the situation of $T = 93$ K and $P = 142$ atm, thus in the supercritical region. As Fig. 1 shows there are well defined solvation shells. The first, starts at a distance of 3.45 Å and ends at about 5.51 Å, with a maximum located at 3.95 Å. For an increased temperature of $T = 151$ K and a corresponding decreased density of 1.05 g/cm^3 (corresponding to $P = 173$ atm) a similar distribution is found with the first solvation shell starting at 3.35 Å and ending at 5.78 Å, with a maximum at 4.05 Å. Spherical integration of this first maximum up to 5.78 Å of the radial distribution gives the coordination of 13 Ar atoms. The distribution functions for the different thermodynamic conditions are also shown in Fig. 1. In the low-density regime the liquid is not well structured and for $\rho = 0.26$ g/cm^3 only one solvation shell is discernible. This is more typical of a gaseous system. The first solvation shell starts at 3.35 Å and ends at 6.50 Å, with a maximum at 4.05 Å and includes only 5 Ar atoms. As the density increases the liquid becomes better structured and in the high-density regime ($\rho = 1.40$ g/cm^3) three solvation shells are easily defined. Interesting, however, the position of the first maximum is relatively stable, and close to 4 Å. Fig. 2 shows the coordination number of the Xe atom for the different thermodynamic conditions. When the Xe atom resides in Ar environment there is a cavity formed that is stable due to the Pauli repulsion and its theoretical radius becomes of interest. It is one ingredient for the possible use of the standard bubble model [4,5,26]. Looking at the beginning of the first peak of the distribution function this radius changes only slightly with the thermodynamic condition. In the cases considered here this value changes between 3.35 and 3.45 Å. Thus we estimate the general size of the cavity formed around the Xe atom as 3.4 Å. Fig. 3 illustrates the situation and depicts the cavity around the Xe impurity. The minimum average distance between Xe and Ar for every thermodynamic condition is thus close to 3.4 Å. Considering the small interaction

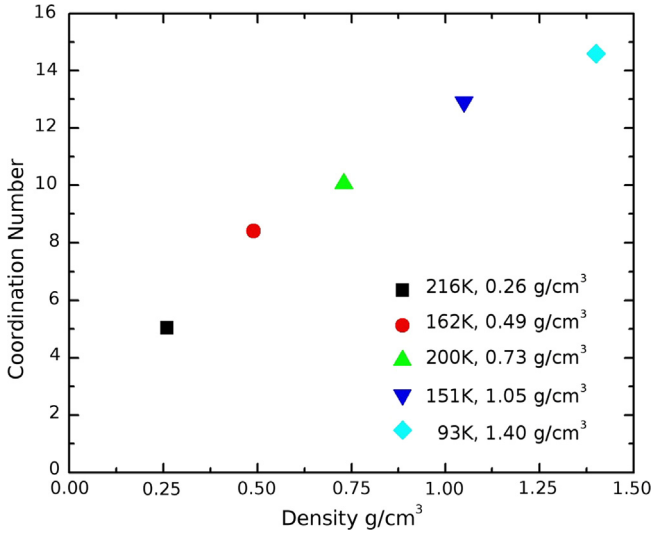

Fig. 2. Calculated coordination number of Xe in the different thermodynamic conditions considered.

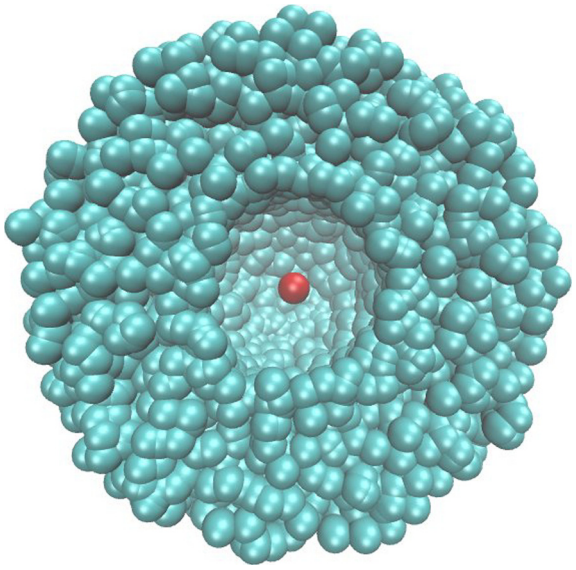

Fig. 3. Illustration of the configuration composed by central Xe atom surrounded by Ar atoms. Different configurations are superimposed to show the central cavity.

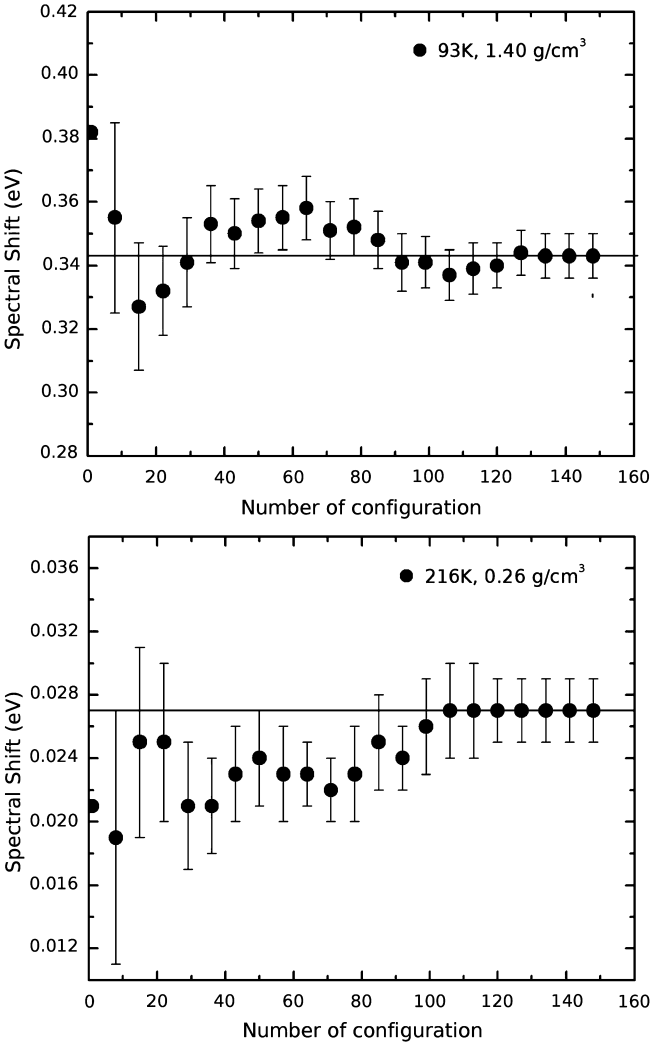

Fig. 4. Convergence of the calculated $^1S_o \rightarrow {}^3P_1$ transition with respect to the number of statistically uncorrelated configurations sampled from the Monte Carlo simulation.

between these two rare-gas atoms the vibrations of the liquid are expected to give a negligible contribution to the shift in the spectral region we are considering.

We now analyze the triplet transition in the thermodynamic condition of $T = 93$ K and $\rho = 1.40$ g/cm^3. In this condition it has been found experimentally [11] that the $^1S_o \rightarrow {}^3P_1$ transition blue shifts by 0.40 eV. In similar condition of $T = 105$ K but much lower pressure of $P \sim 4$ atm, the same transition shifts by 0.36 eV [10]. The gas phase $^1S_o \rightarrow {}^3P_1$ transition of Xe is calculated here using B3LYP/SDD at 149 nm (8.339 eV) in good agreement with the experimental value of 147 nm. Now we consider the transition shift. Using 150 statistically uncorrelated configurations, sampled from the MC simulation at this thermodynamic condition, QM calculations are made for one Xe atom surrounded by 13 Ar atoms. Again, the calculations are made using B3LYP/SDD using the Kohn–Sham approximation [27] with a reference wave function that is anti-symmetric with respect to all valence electrons (Xe and 13 Ar). The average result for the transition energy is then obtained as 8.681 eV $\pm$ 0.080 eV. This corresponds to a blue shift compared to the gas phase of 0.341 $\pm$ 0.080 eV, in good agreement with experiment (0.36–0.4 eV). For comparison the same calculations using the dispersion-corrected B97-D functional [23] give the blue shift value of 0.377 $\pm$ 0.061 eV, similar to the B3LYP results. A larger result of 0.425 $\pm$ 0.077 eV is obtained with the ωB97X-D functional. A population analysis using the B3LYP indicates that there is charge migration of 0.11e from the Ar atoms to the impurity; i.e., the average charge on Xe is calculated as $-0.11e$. This migration reduces with the density of the Ar liquid and in the low-regime case of $\rho = 0.26$ g/cm^3 it is five times less, only $\sim 0.02e$. To verify the statistical convergence of the result Fig. 4 shows the average value as a function of the number of configurations used. About 120 QM calculations are necessary for obtaining converged values. There is an early and interesting theoretical result based on the determination of the excited state Ar + Xe ($^3P_1$) potential. For $T = 105$ K and $\rho = 1.40$ g/cm^3 the resulting value [13] for the shift is found to be 0.41 $\pm$ 0.16 eV, also in good accord with experiment. For the singlet $^1S_o \rightarrow {}^1P_1$ we have obtained a similar but slightly larger blue shift of 0.37 $\pm$ 0.08 eV but the singlet state is apparently not considered in the previous experiments in rare-gas liquids. In addition to the line shift the inclusion of the Xe atom in a liquid environment leads also to an inhomogeneous broadening changing the line profile. The full width at half maximum is obtained from the standard deviation σ using FWHM $= 2\sigma(2\ln 2)^{1/2}$. In this case $\sigma = 0.08$ eV and our estimate

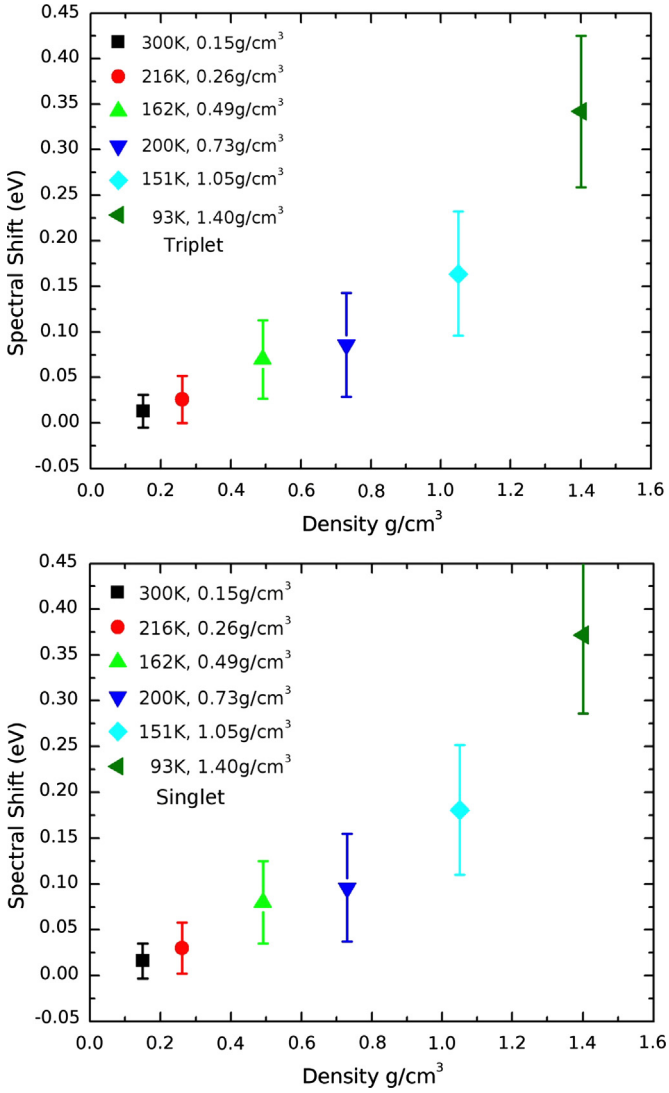

Fig. 5. Variation of the calculated average spectral shift with respect to the liquid density for both the triplet (top) $^1S_o \rightarrow {}^3P_1$ and singlet (bottom) $^1S_o \rightarrow {}^1P_1$ transitions. The variance is also shown.

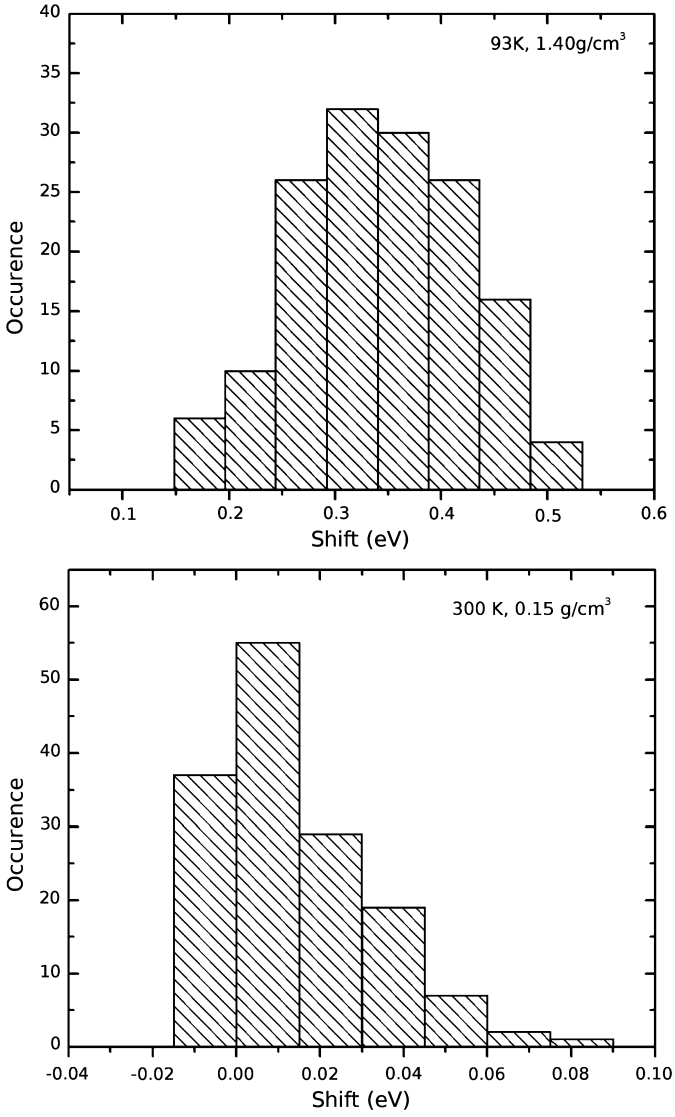

Fig. 6. Histograms showing the distribution of calculated energy shifts. For the low-density case the distribution is asymmetric showing a distinction between the average and the most probable values.

of the FWHM is 0.19 eV. This inhomogeneous broadening is derived from the ensemble of different configurations of the three $p \rightarrow s$ transitions due to the breakdown of the degeneracy of the $5p$ orbital. The $p \rightarrow s$ transition splits with separations that vary between 0.004 eV and 0.10 eV depending on the density.

Having obtained a good description of the spectral shift of the $^1S_o \rightarrow {}^3P_1$ transition in the high-density regime we consider the more systematic analysis of the dependence with the liquid density. This aspect has been studied experimentally and it is found that the shift increases with increased density [11], as expected. The increase, however, is faster than linear and for obtaining this theoretically signifies that the calculation must present a good representation from the low to the high-density regime situation. Then we now report the spectral shift as a function of the density. The results are shown in Fig. 5 and are in complete qualitative agreement with experiments [11]. The error bars shown are, in fact, the variance of the distribution. The statistical error is essentially zero in all cases. This variance is related to the band broadening as discussed above. For $\rho = 1.05$ g/cm^3 a spectral shift of 0.164 eV, corresponding to 1320 cm^{-1} is in very good accord with the experimental value of 1400 cm^{-1} [11,12]. In the moderate case of $\rho = 0.49$ g/cm^3 we obtain a shift of ~ 500 cm^{-1}, still in good agreement with the experimental value close to 400 cm^{-1}. In this spectral region these correspond to an accuracy of less than ~ 2 nm.

In the very low-density regime the situation is typical of a gas and the shift should go to zero. But before this for densities below ~ 0.2 g/cm^3 a more difficult situation appears where the experimental shift is very small and changes sign (red shift) [11,12]. We find for $\rho = 0.26$ g/cm^3 an average blue shift of 200 cm^{-1}. Fig. 4 shows the statistical convergence in this case of low-density situation. However, for the low-density cases the histogram of calculated transition energies is largely non-symmetric and the average differs from the most probable value. The value to be associated with experiment is the most probable value, the maximum of the distribution. For high and intermediate densities this is immaterial. Indeed Fig. 6 shows that for $\rho = 1.4$ g/cm^3 the average is also the most probable value. However, in the case of $\rho = 0.15$ g/cm^3 a different picture emerges. The maximum of the distribution is close to zero and some negative values are also obtained, in agreement with experiment. Figs. 4 and 6 show that the width of the distribution of the calculated values for the spectral shifts is considerably smaller in the low-density regime, due to the decrease in

the interatomic interaction. This explains the increased values of the variance with increased densities as seen in Fig. 5.

4. Summary and conclusions

A combined and sequential use of Monte Carlo simulation and quantum mechanical calculations is a viable procedure for calculation of the structure, electronic properties and spectral changes of atomic impurities in rare-gas in different thermodynamic conditions with varying densities. In this work consistent results are obtained for Xe in Ar environment in all thermodynamic conditions considered. The emphasis here has been the theoretical description of the spectral shift of the Xe $5p \rightarrow 6s$ excitation in Ar environment.

The results reproduce very well the dependence of the spectral shift with density, giving good quantitative results for the low, intermediate and high-density cases.

Acknowledgements

This is work has been partially supported by CNPq, CAPES and FAPESP (Brazil).

References

[1] B. Mennucci, R. Cammi (Eds.), Continuum Solvation Models in Chemical Physics, Wiley, 2007.
[2] S. Canuto (Ed.), Solvation Effects in Molecules and Biomolecules. Methods and Applications, Springer, 2008.
[3] J. Tomasi, Theor. Chem. Acc. 112 (2004) 184.
[4] Y. Takahashi, K. Sano, T. Kinoshita, T. Yabuzaki, Phys. Rev. Lett. 71 (1993) 1035.
[5] F. Dalfovo, Z. Phys. D 29 (1994) 61.
[6] T. Malaspina, K. Coutinho, S. Canuto, J. Chem. Phys. 117 (2002) 1692.
[7] R. Rivelino, B.J.C. Cabral, K. Coutinho, S. Canuto, Chem. Phys. Lett. 407 (2005) 13.
[8] L. Modesto-Costa, K. Coutinho, P.K. Mukherjee, S. Canuto, Phys. Rev. A 83 (2011) 042515.
[9] T.L. Fonseca, K. Coutinho, S. Canuto, Phys. Chem. Chem. Phys. 12 (2010) 6660.
[10] B. Raz, J. Jortner, Proc. R. Soc. Lond. Ser. A 317 (1970) 113.
[11] I. Messing, B. Raz, J. Jortner, J. Chem. Phys. 66 (1977) 2239.
[12] J.M. Rupin, M. Morlais, S. Robin, C. R. Acad. Sci. Ser. B 265 (1967) 1177.
[13] M.J. Saxton, J.M. Deutch, J. Chem. Phys. 60 (1974) 2800.
[14] D.M. Heyes, The Liquid State. Applications of Molecular Simulations, John Wiley, New York, 1998.
[15] M.P. Allen, D.J. Tildesley, Computer Simulation of Liquids, Clarendon Press, 1987.
[16] L. Verlet, J.J. Weis, Mol. Phys. 24 (1972) 1013.
[17] K. Coutinho, S. Canuto, DICE (Version 2.9): A General Monte Carlo Program for Liquid Simulation, University of São Paulo, 2009.
[18] E. Runge, E.K.U. Gross, Phys. Rev. Lett. 52 (1984) 997.
[19] A.D. Becke, J. Chem. Phys. 98 (1993) 5648.
[20] C. Lee, W. Yang, R.G. Parr, Phys. Rev. B 37 (1998) 785.
[21] P. Fuentealba, H. Preuss, H. Stoll, L. von Szentpaly, Chem. Phys. Lett. 89 (1982) 418.
[22] A. Nicklass, M. Dolg, H. Stoll, H. Preuss, J. Chem. Phys. 102 (1995) 8942.
[23] S. Grimme, J. Comp. Chem. 27 (2006) 1787.
[24] J.-D. Chai, M. Head-Gordon, Phys. Chem. Chem. Phys. 10 (2008) 6615.
[25] M.J. Frisch, et al., Gaussian 09, Revision A.1, Gaussian, Inc., Wallingford, CT, 2009.
[26] A.N. Sil, S. Canuto, P.K. Mukherjee, Adv. Quantum Chem. 58 (2009) 115.
[27] W. Kohn, L.J. Sham, Phys. Rev. A 140 (1965) 1133.